A STUDY OF PARAMETERS INFLUENCING THE HYGRIC BEHAVIOR OF INSULATED SLOPED ROOFS WITHOUT AIR BARRIER

Arnold Janssens **Hugo Hens, Ph.D.** **Ann Silberstein, Ph.D.**

ABSTRACT

Previous research by the authors (Janssens et al. 1992) revealed that airflows, both exfiltrating through an envelope and flowing by stack effect in and around thermal insulation, have a negative influence on the thermal and hygric performance of insulated sloped roofs. Therefore, a new guideline was proposed to design pitched roofs with cathedral ceilings in which the most important rule is to achieve airtightness by installing an airtight layer (air barrier) at the inside of the thermal insulation. This, however, demands excellent workmanship. As that is not always guaranteed, it is of interest to explore solutions less dependent on practice to prevent moisture problems. Different solutions are tested in a series of hot box-cold box condensation experiments where the hygrothermal behavior of three sloped roofs, typical of French roof construction, is simultaneously monitored. The roof layouts reflect the use of different measures to prevent interstitial condensation: a vapor-retarding internal lining, a vapor-open underlay, and a vapor-retarding insulation material. The experimental results are discussed and related to modeling predictions, which gives a better understanding of the parameters influencing the condensation phenomenon.

INTRODUCTION

Former experimental work by the authors showed that a tiled roof insulated between the rafters is, above all, an air-permeable construction generating a complex, mixed pattern of airflows (Hens 1992, 1994; Janssens et al. 1992). Because air carries vapor and enthalpy, more heat and moisture may be transported in and through a roof than according to conduction and diffusion theories. Energy efficiency and hygric performance appear to be largely determined by air exfiltration through the roof and stack flow in and around the insulation layer. Those understandings ended in the formulation of two basic performance rules for tiled roofs with cathedral ceilings: (1) realize airtightness and (2) prevent air rotation in and around thermal insulation. Only when the basic rules are fulfilled does it make sense to impose second-level performance rules: (3) control diffusion and (4) use a vapor-open and/or capillary underlay. Application of these guidelines to tiled roofs with cathedral ceilings leads to a so-called "compact roof" design: the insulation layer is sandwiched between a wind barrier (the underlay) and an airtight layer. To avoid air layers on either side of the insulation layer, the cavity between the rafters is completely filled with insulation. The use of a PE foil as an air and vapor barrier, mounted continuously beneath a mineral wool filling, has proven to be the best choice to ensure the sound hygric performance of a cathedral roof (Hens 1992). However, installing and sealing a PE foil as an airtight system implies some disadvantages. First, it creates an additional step and cost in the construction work. It also demands excellent workmanship: with some construction methods it is even impossible to achieve airtightness. This is particularly true for the roof layout promoted in France and studied in this work. Therefore, it is of interest to explore solutions to prevent moisture problems in sloped roofs without a PE air barrier.

OBJECTIVES

The characteristic feature of the roof construction promoted in France is the use of a metallic rail system, suspended from the rafters by means of metal spacers, to attach the internal lining. Apart from the acoustical and practical benefits, the system offers some obvious advantages for energy efficiency. Due to the spacers, the installed insulation thickness is independent of the constructional rafter height. By compressing the mineral wool slabs underneath the rafters, the effect of thermal bridging is diminished. As a result, the thermal resistance of the roof increases. However, with the use of the rail sys-

Arnold Janssens is a researcher and Ph.D. student and **Hugo Hens** is a professor and head of the Laboratory of Building Physics at the Catholic University of Leuven, Belgium. **Ann Silberstein** is a researcher at the CRIR Isover Saint-Gobain, Rantigny, France.

tem, it is difficult to finish a foil underneath the insulation as an airtight layer. A possible alternative is to mount a gypsum board internal lining as an air retarder. Janssens et al. (1992) analyzed this choice in a hot box-cold box experiment in combination with a vapor-permeable underlay and partial filling of glass wool. The results looked promising: no interstitial condensation was observed against the underlay.

This paper analyzes other measures to prevent moisture problems in tiled roofs with a gypsumboard as an air retarder. The first is to paint the gypsumboard with an acrylic paint system to obtain a better air- and vaportightness of the internal lining. The test analyzes whether this step is sufficient to avoid interstitial condensation, even in combination with a common, vaportight underlay. A second measure is to apply a vapor-permeable foil as underlay. Would this still reduce condensation when the rafter cavity is completely filled with glass wool? Finally, the use of an air- and vapor-retarding, rigid insulation material such as expanded polystyrene is investigated. The experiment verifies whether this choice results in better hygric and thermal performance of the roof than when glass wool is applied.

EXPERIMENTAL METHOD

The test roofs are mounted in a frame that is enclosed between a hot box and a cold box, simulating the inside and outside climates. A cooling or heating device and free evaporation of saturated salt solutions maintain, respectively, the temperature and relative humidity in each box at a constant level. A fan group connected to the hot box may install a constant air pressure difference over the test roofs. This forces warm, humid air to exfiltrate through the test roofs to the cold box. A fan group in the cold box creates a constant airflow parallel to the tile layers, thus simulating the influence of the wind.

With each experiment, three different roof layouts are measured simultaneously. A test roof is constructed as a fragment of a wood-frame roof with dimensions (length by width) of 2.15 m by 0.78 m (7 ft by 2.5 ft), roof slope 60 degrees, rafter section 40 mm by 200 mm (1.6 in. by 8 in.), and distance between centerlines of 0.37 m (1.2 ft). The different parts of the roof sections are conceived to be detachable to follow their weekly change of weight. On each layer surface of the three test roofs and at different heights, devices are installed to measure temperatures, heat flow rates, air pressures, and tracer gases. Temperatures, heat flows, and relative humidity are measured continuously by datalogging. Air pressures and airflow rate are measured weekly. Moisture migration in the roofs is mapped by opening the boxes each week and weighing all composing parts of the three roof sections.

The experiment is developed in three stages, during which exfiltration becomes more important. During a first "diffusion" stage, no air pressure difference is installed. During a second stage, a constant air pressure difference is maintained, creating exfiltration through the roofs. During the third stage, the exfiltration rate is increased by doubling the air pressure difference. Table 1 lists the averaged boundary conditions measured during the different stages. The cold box reflects January-averaged conditions in Belgium. The hot box simulates conditions in inhabited attic spaces, as derived from a measuring campaign in 20 loft apartments (Hens 1992).

TABLE 1 **Averaged Measured Boundary Conditions**

Duration	Stage 1 11 weeks	Stage 2 8 weeks	Stage 3 8 weeks
ΔPa (Pa/In. of Hg)	0	4.4 (1.3E-3)	9.9 (2.9E-3)
θ hot box (°C/°F)	19.8 (67.6)	17.9 (64.2)	18.0 (64.4)
$RH_{hot\ box}$ (%)	43	60	57
$\theta_{cold\ box}$ (°C/°F)	1.6 (34.9)	1.2 (34.2)	2.2 (36.0)
$RH_{cold\ box}$ (%)	80	88	91

TEST ROOFS

Layout

The three roof layouts, presented in Figure 1, reflect the use of different measures to prevent interstitial condensation: a vapor-retarding internal lining (roof 1), a vapor-open underlay (roof 2), and a vapor-retarding insulation material (roof 3).

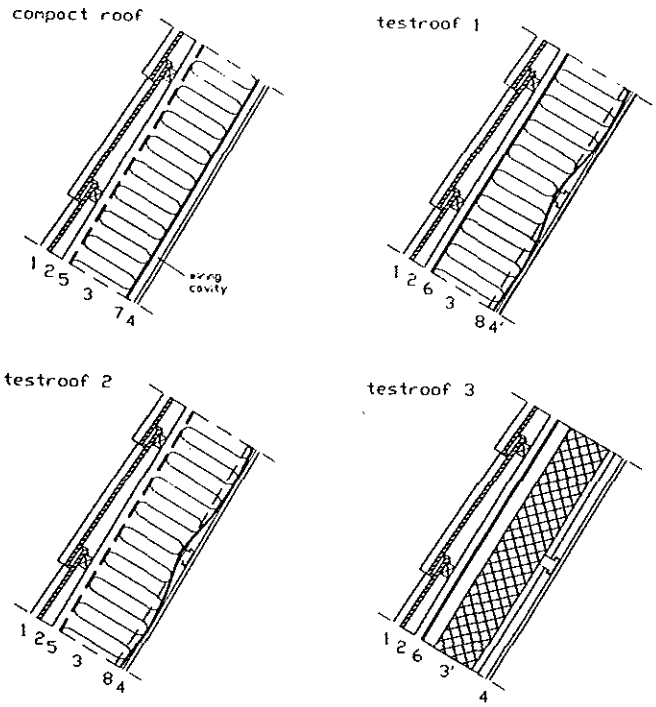

Figure 1 Layout of compact roof and test roofs, with tiles (1), laths and battens (2), glasswool blanket (3), expanded polystyrene board (3'), gypsum board (4), painted gypsum board (4'), vapor-permeable underlay (5), vapor-retarding underlay (6), polyethylene foil (7), and kraftpaper (8).

Roof 1 The gypsumboard lining is suspended from the rafters by means of a metal U-profile system. The board is painted with a primer and two layers of acrylic paint. Because the board functions as an air retarder, joints are finished as airtight as possible. Horizontal joints between boards are caulked with a reinforced gypsum filler. Joints between boards of different test roofs or between board and box are tightened with silicone sealing. The roof is insulated with low-density glass wool slabs with kraft facing. The slabs fill the complete, 20-cm-thick cavity between internal lining and underlay. They are installed according to common practice: joints between different slabs are not taped. A dismountable frame, screwed on top of the rafters, contains the vapor-tight underlay (V-T): a bituminous-impregnated membrane of polypropylene fibers. It is assembled in three parts with two horizontal overlaps. Finally, the roof covering consists of water-repellent concrete tiles, double lock type; lathes and battens connect tiles and underlay.

Roof 2 The layout is largely the same as that of roof 1, except for two differences. The gypsumboard is not painted and, instead of a vapor-tight underlay, a vapor-open underlay (V-O) is applied: a spun-bonded polyethylene membrane, consisting of two parts with one horizontal overlap in the middle of the roof slope.

Roof 3 Also in roof 3, the layout shows two differences in comparison with roof 1. The gypsumboard is not painted. Instead of glass-wool slabs, a rigid, vapor-retarding insulation material is applied: expanded polystyrene board (MPS). Because of the metal rail system, it is impossible to avoid air layers between this type of insulation material and the internal lining. In this case, a 4-cm-wide air cavity is left on either side of the MPS layer. The boards are sawed to match the space between the rafters as precisely as possible, but, to simulate common practice, joints between insulation boards and rafters are not sealed.

Material Properties

Measurements were made to determine the thermal conductivity, vapor permeance, and air permeance of each composing material. They are listed in Table 2. For most materials, two values of the vapor diffusion thickness are measured: one "dry" and one "wet" value. The vapor-retarding properties of the painted gypsumboard particularly diminish at higher relative humidities. To estimate the vaportightness of the layers as they appear in the roofs, discontinuities included an equivalent diffusion thickness (μd_{eq}) is calculated with a two-dimensional stationary diffusion model. The values illustrate the effect of diffusion leaks as joints, overlaps, and perforations. The kraftpaper back of the glass wool slabs clearly loses its function as a vapor retarder; the vapor resistance diminishes with factor 8. The thermal properties allow one to calculate the overall heat transfer coefficient (U) of the three test roofs. Roofs 1 and 2 have the same U-factor: 0.17 W/(m²·K) (0.029 Btu/[h·ft²·°F]). The U-factor of roof 3 is higher: 0.33 W/(m²·K) (0.057 Btu/[h·ft²·°F]).

TABLE 2 Material Properties

Thermal Properties	Thickness mm (in.)	Density ρ kg/m³ (lb/ft³)	λ W/(m·K) (Btu·in./(h·ft²·°F))	R m²·K/W (ft²·h·°F/Btu)
Gypsumboard	9.5 (0.37)	762 (47.6)		0.05 (0.28)
Glasswool	200 (7.87)	16.0 (1.0)	0.035 (0.24)	
Expanded PS	120 (4.72)	9.3 (0.6)	0.049 (0.34)	
Tiles				*0.06 (0.34)*

	Vapor Diffusion Thickness (Vapor Permeance)			Air Permeance
Mass Transfer Properties	RH %	μd (δ/d) m (perm)	μd_{eq} (δ_{eq}/d) m (perm)	K_a kg/(m²·s·Pa)
Gypsumboard	28	0.14 (23.0)	**0.1 (32.3)**	$7.7E\text{-}7 \cdot \Delta p^{-0.02}$
	92	0.04 (80.7)		
+ paint	26	2.30 (1.4)	**2.3 (1.4)**	$4.6E\text{-}7 \cdot \Delta p^{-0.06}$
	92	0.34 (9.5)		
Kraftpaper	*54**	*4.95 (0.7)*	**0.6 (5.4)**	
Glasswool			*0.24 (13.4)*	
Expanded PS	28	2.57 (1.2)	**2.0 (1.6)**	$1.3E\text{-}4 \cdot \Delta p^{-0.10}$
	92	2.03 (1.6)		
V-O underlay	26	0.05 (64.5)	**0.012 (269)**	$1.8E\text{-}6 \cdot \Delta p^{-0.03}$
	92	0.012 (269)		
V-T underlay	26	33.4 (0.1)	**5.5 (0.6)**	$9.9E\text{-}7 \cdot \Delta p^{-0.07}$
	92	17.7 (0.2)		
Tiles			*0.12 (26.9)*	

*normal = measured; bold = calculated; italic = earlier work (Janssens et al. 1992; Hens et al. 1986)

MEASURING RESULTS

Thermal Performance

Stage 1 To judge the thermal performance of the test roofs, the conductive heat fluxes are measured at three different heights along the surface of the internal lining. A typical example of measured heat fluxes is the averaged flows for roof 3 during the first stage:

W/m^2 (Btu/[h·ft^2])	Top	Middle	Bottom
Heat flow rate	7.7 (2.4)	14.7 (4.7)	33.6 (10.7)

When no air pressure difference is imposed, heat flow through the roofs is dominated by stack flow in and around the insulation layer. Stack flow is linked to temperature differences, and results in airflows rotating in and around the insulation layer. Air is heated on the warm side of the insulation layer, rises along the surface, and infiltrates through the insulation or through joints to the cold side. Here the air cools down again, drops along the cold surface, and flows back to the warm side. This explains the higher heat flow rates, measured at the bottom of the roofs. If the resistance against stack flow is small, it may lead to a significant increase in energy loss. To quantify this influence, effective U-factors are derived from the measured heat fluxes: the surface-weighted average of the heat flow rates is divided by the measured temperature difference over the roofs. Table 3 lists this value and compares it to the calculated U-factor, which takes only heat conduction into account. In the roofs with glass wool insulation, the effect of stack flow is limited to an increase of 40% in roof 2. In the roof with MPS insulation, on the other hand, the effect is considerable: the energy loss through the roof is three times higher than when stack flow would be eliminated. Apparently, the presence of even small joints between insulation board and rafters is sufficient to connect the air layers on both sides of the insulation, thus creating a flow path for stack flow.

Table 3 **Thermal and Hygric Performance**

		ROOF 1	ROOF 2	ROOF 3
U-Factor	W/(m^2·K) (Btu/(h·ft^2·°F))			
	U_{calc} =	0.17 (0.029)	0.17 (0.029)	0.33 (0.057)
	U_{eff} =	0.16 (0.028)	0.24 (0.042)	0.98 (0.172)
$(U_{eff} - U_{calc})/U_{calc}$ =		-7%	+40%	+198%
Condensation Rate	g/(m^2·day)(gr/(ft^2·day))			
Stage 1:	avg =	1.3 (1.9)	0.7 (1.0)	3.6 (5.2)
	r^2 =	0.60	0.23	0.94
Stage 2:	avg =	18.6 (26.7)	17.8 (25.5)	4.1 (5.9)
	r^2 =	0.94	0.89	0.90
Stage 3:	avg =	34.4 (49.3)	7.0 (10.0)	12.6 (18.1)
	r^2 =	0.95	0.57	0.99

Stages 2 and 3 Once an air pressure difference is imposed on a construction, heat fluxes are influenced by air exfiltration. Therefore, the measured heat fluxes are closely connected with the actual amount of air flowing through the roofs. They give an indication of both the conductive and the ventilative heat losses. Because of this, it is impossible to derive a physically meaningful U-factor.

Hygric Performance

During the first measuring period, significant amounts of condensation against the underlay were observed only in roof 3. Here a small gutter was installed to collect the pouring condensate. During the second and third stages, however, all roofs suffered from moisture. From the moment air exfiltration became active, condensation occurred in roofs 1 and 2 as some spread drops between the underlay and the glass wool. After some weeks, the drops ran down, wetting the studs and glass wool slabs at the bottom. To measure the amount of runoff in these roofs, a gutter also was installed in roofs 1 and 2 during the third stage.

Figure 2 shows the measured weight increase due to condensation in the three test roofs. Table 3 lists the results of a least-squares fit between measured condensation and time. The "condensation" amounts taken into account contain the measured weight increase of the underlay frames and insulation and the accumulated weight of the water collected by the gutters, with a correction for the hygroscopic wetting of the wooden parts in the frame.

On the basis of the test results alone, no distinction can be made between a "good" or a "bad" construction. None of the roofs seems to provide a sufficient solution to prevent condensation. Still, some points of similarity between the hygric behavior of the three roofs are striking. The roofs with glass wool insulation, roofs 1 and 2, perform well during the first measuring period. Afterward, though, when air exfiltration is imposed, they too

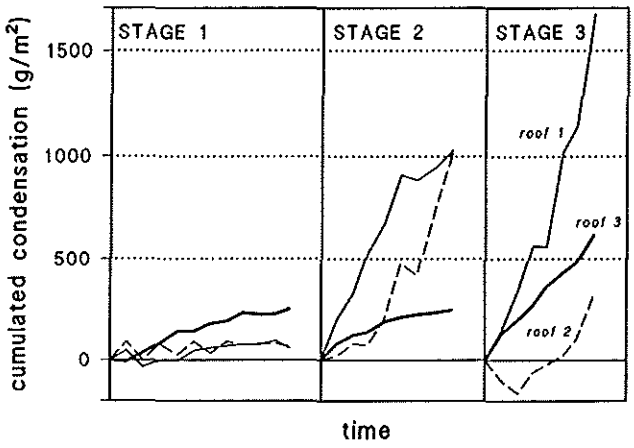

Figure 2 Measuring results: Cumulated condensation as a function of time in the test roofs.

suffer from moisture. Almost as a general trend, an increasing air pressure difference results in a higher condensation rate. This indicates that, for these test roofs, hygric performance is closely linked to air transport. The remarkable thing is that, once air exfiltration is active, roof 3 shows less condensation than roof 1, although it obviously behaves worse without exfiltration (stage 1). The hygric behavior of the second roof (vapor-open underlay) is different from that of the others. Although condensation in roof 2 is clearly present, it is not linked to air exfiltration in the same way as in the other roofs. It also shows large variations: the same boundary conditions may cause drying during one week and during the next, condensation.

Airtightness

The strong influence of air exfiltration on the hygric behavior of the test roofs is indicative of a lack of airtightness. Because the air permeance of the gypsumboard is sufficiently low to make a good air retarder, only a lack of continuity of the internal lining may explain air leakage through it. After an inspection of the roofs during the second stage, a longitudinal shrinkage crack was discovered between the top of the gypsumboard and the box frame, with a relative length of 0.46 m/m^2 (1.7 $in./ft^2$). The appearance of these cracks during the experiment provided the opportunity to study their influence.

During stage 3, airflow in and through the roofs was mapped by means of tracer gas equipment. Two different measurements were performed. First, a constant concentration of tracer gas was maintained in the cold box to evaluate the windtightness of the roofs. Air was continuously sampled in the hot box, between insulation and gypsumboard, and between insulation and underlay in the three roofs. The results revealed cold air infiltration in roof 2 between insulation and underlay, with a rate of approximately 0.38 L/s (48 ft^3/h) at the time of measurement. Infiltration in the other roofs was not detected. This might explain the difference between the effective U-factors measured in roofs 1 and 2; both roofs still had the same insulation thickness.

The objective of the second measurement was to observe differences between the airtightness of the three roofs. This time, a constant concentration was built up in the hot box, while air was sampled in the cold box and between insulation and gypsumboard of the different roofs. All roofs demonstrated the same immediate response to a changing concentration in the hot box, indicating no difference in air leakage between the roofs. The averaged air exfiltration rate amounted to 0.92 $L/(m^2 \cdot s)$ (10.9 $ft^3/[ft^2 \cdot h]$) at the time of measurement. On the basis of the measured air permeances of the roof-composing layers (without cracks), an exfiltration rate of only 6 $mL/(m^2 \cdot s)$ (0.07 $ft^3/[ft^2 \cdot h]$) can be expected. Due to the presence of cracks, air exfiltration through the roofs increased by a factor of 150.

INTERPRETATION

Calculation Models

The use of calculation methods can be helpful in the interpretation of measuring results. Here, they are applied in two different ways. On one hand, a model is used to reproduce the measuring results and to explain the parameters influencing them in detail. For this purpose, the calculation code "Konvek" is applied (Hens et al. 1986; Hens et al. 1992). "Konvek" is a two-dimensional stationary model for the combined calculation of air, heat, and vapor flow. Diffuse, orifice, as well as channel flow may be included, with the air pressure as potential. This means all types of airflows, except rotative stack flow, are taken into account. The model allows one to describe a construction in terms of air-permeable materials, air-permeable layers, air cavities, and leaks. The test roofs are modeled as listed in Table 4.

On the other hand, a model can be applied to stress the large deviations between the results of the calculation and the test. This methodology emphasizes the importance of the phenomena not taken into account by the model. Two one-dimensional models serve the latter purpose. "One-dimensional" means that the calculation takes into account only heat and mass flows perpendicular to the

TABLE 4 Layout of Roofs in "Konvek"

			Dimensions: Thickness or Width in mm (in.)		
Layer	Defect	Location	Roof 1	Roof 2	Roof 3
Gypsumboard	crack	top	varying	varying	varying
	cavity		2 (0.1)	2 (0.1)	40 (1.6)
Glasswool	air permeable		200 (8)	200 (8)	
MPS	air permeable				120 (4.7)
	joint	top			5 (0.2)
		middle			2 (0.1)
		bottom			2 (0.1)
	cavity				40 (1.6)
Underlay	joint	top	varying	varying	varying
		bottom	1 (0.04)	1 (0.04)	1 (0.04)
	overlap	middle		x	
		65 cm (25.6 in.)	x		x
		155 cm (61 in.)	x		x
	cavity		25 (1)	25 (1)	25 (1)
Tiles	air permeable		x	x	x

construction surface. With this hypothesis, the results represent for most constructions only part of their real behavior.

The "Glaser scheme" assesses the condensation rate without taking airflows into account (Glaser 1959). Heat is transferred by conduction, vapor by diffusion. The amount of condensation is calculated according to Equations 1 and 2:

$$\theta_c = \theta_e + (\theta_i - \theta_e) \cdot R_c^e / R_{tot} \quad (1)$$

$$g_c = \frac{p_i - p_{sat,c}}{Z_i^c} - \frac{p_{sat,c} - p_e}{Z_c^e}. \quad (2)$$

The "diffusion-convection scheme" assesses the influence on condensation of airflows perpendicular to the envelope. All materials are assumed to be permeable to air. In addition to conduction and diffusion, the calculation takes into account heat and vapor carried by the air. Condensation is calculated according to Equations 3 and 4:

$$\theta_c = \theta_e + (\theta_i - \theta_e) \cdot \frac{1 - \exp(g_a \cdot c_a \cdot R_c^e)}{1 - \exp(g_a \cdot c_a \cdot R_{tot})} \quad (3)$$

$$g_c = g_a \cdot \xi_a \cdot \left[\frac{p_i - p_{sat,c}}{1 - \exp(g_a \cdot \xi_a \cdot Z_i^c)} - \exp(g_a \cdot \xi_a \cdot Z_c^e) \cdot \frac{p_{sat,c} - p_e}{1 - \exp(g_a \cdot \xi_a \cdot Z_c^e)} \right] \quad (4)$$

Modeling Predictions

Influence of Exfiltration Condensation rates in the three roofs are calculated according to the Glaser and diffusion-convection schemes. The averaged boundary conditions of each measuring period are introduced in the models. The material properties used are corrected for air and diffusion leaks. For the calculation of the equivalent air permeance of gypsumboard, the assumption has been made that a crack with a width of 0.75 mm (0.03 in.) dominates the airflow through it. Results are listed in Table 5.

Because no air exfiltration is active during the first stage, the Glaser predictions are of the same order of magnitude as the measured condensation rates. The calculations for stages 2 and 3 underestimate condensation in comparison with the test results. This divergence emphasizes the importance of the mechanism not taken into account by the calculation: air exfiltration. However, the diffusion-convection scheme, which does take exfiltration into account, overestimates the condensation rates. How to explain this?

TABLE 5 **One-Dimensional Modeling Predictions**

Condensation Rate		Roof 1	Roof 2	Roof 3
g/m²·day) (gr/(ft²·day))				
Glaser:	Stage 1	1.0 (1.4)	no condensation	1.6 (2.3)
	Stage 2	2.6 (3.7)	no condensation	3.9 (5.6)
	Stage 3	2.1 (3.0)	no condensation	3.2 (4.6)
Dif.-con.:	Stage 2	112.5 (161.4)	100.4 (144.0)	97.6 (140.0)
	Stage 3	151.4 (217.2)	130.7 (187.5)	134.4 (192.8)

Because the diffusion-convection scheme is a one-dimensional model, it only assesses the influence of airflows in one direction. In reality though, air follows a complex path through a construction, searching for discontinuities such as cracks, joints, overlaps, etc. ... The deviations between the diffusion-convection predictions and the test results show the significance, not only of the exfiltration rate, but also of the exact flow path on the hygric behavior of a roof. To come to a detailed understanding of the importance of small defects, a calculation with a two-dimensional model is, therefore necessary.

The Influence of Cracks As the tracer gas measurement already proved, cracks destroy the airtightness of a gypsumboard lining. To quantify this influence, the airflow rate through the cracks is calculated according to the well-known theories of fluid flow in ducts. From these values, the total airflow through a gypsumboard with a crack length of 0.46 m/m² (1.7 in./ft²) is derived. Both the influence of the crack width (d_{crack}) and the presence of screw holes are investigated.

- gypsumboard without cracks:
  6 mL/(m²·s) (0.07 ft³ /[ft²·h])
- gypsumboard, 2 holes Ø mm (0.12 in.):
  33 mL/(m²·s) (0.38 ft³ /[ft²·h])
- gypsumboard, d_{crack} = 0.5 mm (0.02 in.):
  252 mL/(m²·s) (2.97 ft³ /[ft²·h])
- gypsumboard, d_{crack} = 1 mm (0.04 in.):
  1044 mL/(m²·s) (12.3 ft³ /[ft²·h])

The values listed are calculated at an air pressure difference of 10 Pa. They confirm that a gypsumboard with even small defects loses its function as an air retarder. How drastically would this effect change the hygric behavior of the roofs? To answer this, the test roofs are designed using the "Konvek" model. The influence of a varying crack width on the global condensation rate is examined for the averaged boundary conditions measured during stage 2. Figure 3 shows the results for the roofs insulated with glass wool (roofs 1 and 2). Both the orders of magnitude of the measured condensation rates, as the general trend of the test results, are reproduced by the calculations. When the internal lining is not perfectly airtight, neither a vapor-tight finish such as the coat in roof 1 nor a vapor-open underlay such as the one in roof 2 can guarantee a sound hygric performance of the roof. After all, both measures manipulate the transport of vapor by diffusion but, because air-

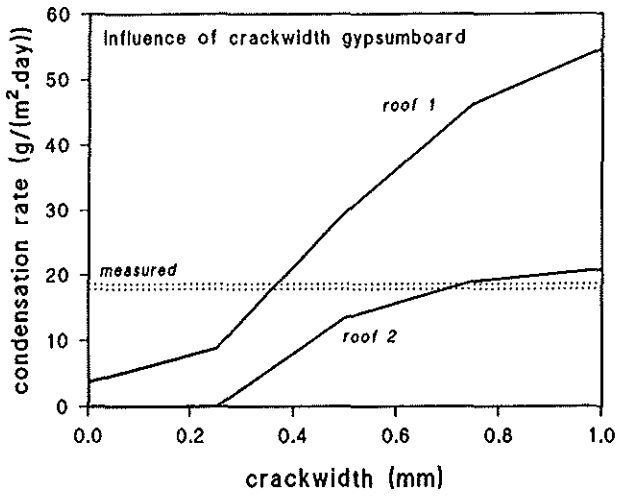

Figure 3 *Modeling results: Influence of airtightness on the condensation rate on roofs 1 and 2.*

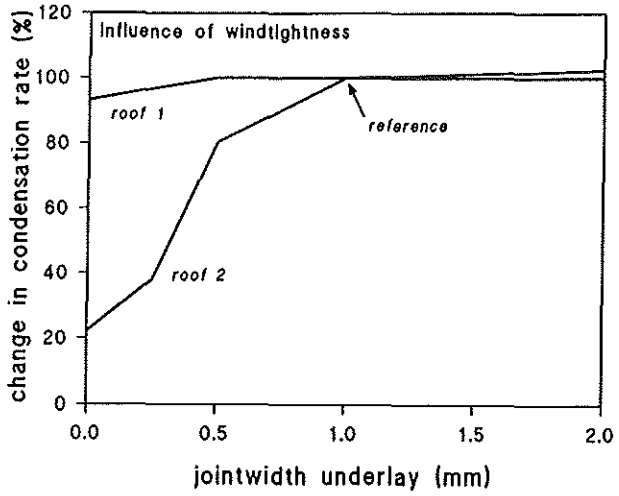

Figure 4 *Modeling results: Influence of windtightness on the condensation rate on roofs 1 and 2.*

flows are able to transfer larger amounts of vapor than diffusion, they fail when exfiltration is active. Once the width of a crack is larger than a critical value, the condensation rate increases fundamentally with crack width and, consequently, with exfiltration rate. From this point of view, roof 2 seems more forgiving toward defects than roof 1: no condensation is predicted for crack widths smaller than 0.25 mm (0.01 in.). With larger cracks, the condensation reaches a constant level: when the airtightness of the gypsumboard diminishes, other layers—such as the underlay—adopt its function of air barrier, hence limiting exfiltration and condensation.

The Influence of Windtightness The tracer gas measurement proved that, even in roofs with a stuffed cavity, infiltration through the underlay is a reality. Possible leaks are situated at the overlaps in the underlay and at the joints between the underlay frame and rafters. The influence of the airtightness of the underlay frame on the condensation rate in the roofs is analyzed with the model "Konvek" for stage 2. Figure 4 shows the change in condensation rate as a function of the upper joint width of the frame. The change is expressed as a percentage of the condensation amount in the reference case, that is, a joint width of 1 mm (0.04 in.). In all cases shown, the crack width in the gypsum board is also 1 mm. Both roofs behave in different ways. While roof 1 shows hardly any response, roof 2 is sensitive to changes in the airtightness of the underlay frame. Condensation varies from 20% to 100%. This result might explain the fluctuations of the measured condensation rates in roof 2. Every week the underlay frame is dismounted, weighed, and mounted again. This method probably affects the windtightness of the roof, thus influencing its hygric behavior.

The Influence of Natural Convection The heat flux measurements revealed that natural convection is most active in the roof with polystyrene insulation (roof 3). Air rotates around the insulation board through channels and leaks, carrying heat and vapor. The consequences on energy efficiency have been explained: three times more heat is transferred through the envelope than if natural convection would be prevented. The influence on the hygric performance of the roof is clear when comparing the test results for stage 1 with the Glaser predictions. The calculated condensation amount is less than half the measured one. In reality, vapor is transferred around the polystyrene board instead of diffusing through it, so its function as a vapor retarder is short-circuited. This is why roof 3 suffers more from moisture than the other roofs during the first measuring period. How to explain its better hygric behavior during the following stages?

As a consequence of the poor thermal performance of the roof, the temperatures at the underlay rise. During stage 2, for instance, the average measured temperature at the underlay was 9.3°C (48.7°F) in roof 3, while it was only 5.2°C and 4.2°C (41.4°C and 39.6°F) in roofs 1 and 2, respectively. Now, the vapor carried by exfiltration condenses against the underlay if the temperature of the surface is lower than the dew point of the air. The bigger the difference between surface and dew-point temperatures, the bigger the condensation rate. Because the temperatures at the underlay in roof 3 are significantly higher than those in the other roofs, the exfiltration of humid air ends in lower amounts of condensation. Figure 5 shows a comparison between calculations for stage 2 with the diffusion-convection scheme and the model "Konvek." Both models overestimate condensation in roof 3 in comparison with the measuring results. This deviation shows the importance of the phenomenon taken into account by neither of the calculations: natural convection. By replacing Equation 3 with the measured temperature at the underlay, the effect of natural convection can be quantified with the diffusion-convection scheme. The result of this calculation, plotted in Figure 5, is of the same order of magnitude as the measurements. The better hygric behavior of